

# Modulated Photocurrent Measurements on Icosahedral Cluster Solids: Boron-Rich Solids and Aluminum-Based Quasicrystals

Masatoshi Takeda,<sup>1</sup> Ryuji Tamura,<sup>1</sup> Yoshiko Sakairi, and Kaoru Kimura

*Department of Materials Science, University of Tokyo, Tokyo 113, Japan*

Received April 14, 1997; accepted April 28, 1997

Modulated photocurrent measurements were performed on amorphous boron,  $\beta$ -rhombohedral boron, and Al–Pd–Re quasicrystal. For the quasicrystal, this is the first report on photoconductivity. The data obtained for amorphous boron are analyzed by a typical model which assumes interband photocarrier generation and trap-limited conduction. Those for  $\beta$ -rhombohedral boron and the quasicrystal are analyzed by a modified model which takes account of two excitation processes for carriers: (i) photoexcitation directly to conduction (or valence) band and (ii) that to localized states followed by thermal excitation into conduction (or valence) band. The results indicate that the localized states significantly contribute to photoconduction. The existence of large densities of localized states is suggested both for  $\beta$ -rhombohedral boron and quasicrystals. © 1997 Academic Press

## INTRODUCTION

The discovery of superconductivity in alkali-metal-doped  $C_{60}$  (1) has stimulated a great interest in related materials called "Cluster Solids." Boron and aluminum tend to form 12-atom icosahedral clusters in solids; the former exists in boron-rich semiconductors and the latter exists in aluminum-based quasicrystals (2).

Icosahedral quasicrystals have been found in numerous metallic alloy systems, mainly aluminum-based systems. Although they consist of metal atoms, their electrical conductivity is extremely low compared with that of crystalline and amorphous phases, and the conductivity decreases with decreasing temperature. It is considered that such unusual behavior is attributed to the existence of a pseudogap in the electron density of states at the Fermi level and the localization tendency of electrons near the Fermi level (3). Whereas electronic properties of quasicrystals have been intensively investigated, they have not been fully understood because of the difficulties in theoretical study resulting from the lack of

translational symmetry. Since the energy band scheme for the quasicrystals is similar to that for amorphous semiconductors, observation of photoconductivity in the quasicrystals is strongly expected and will give us significant information about their electronic structure and transport mechanism. On the other hand, as we reported previously (4), boron-rich solids have structural similarity to quasicrystals. It is therefore important to compare their physical properties to clarify the relationship between boron-rich solids and aluminum-based quasicrystals as the "Icosahedral Cluster Solids" (2, 5).

The modulated photocurrent (MPC) method is a very sensitive measurement and is extensively applied to determine an energetic distribution of the localized states both in crystalline and amorphous semiconductors (6–9). In the present paper, we discuss the photocarrier generation process, the transport process, and the localized states in the energy gap on the basis of the results measured by means of the MPC method.

## EXPERIMENTAL PROCEDURE

Amorphous boron film with a thickness of 1.3  $\mu\text{m}$  was prepared by an electron-beam evaporation technique (10). Coplanar geometry Al electrodes with a 1 mm spacing were evaporated onto the surface of the film. A single crystal of  $\beta$ -rhombohedral boron (5N) produced by Eagle–Picher Inc. was mechanically polished with diamond (finest grade 1/4  $\mu\text{m}$ ) for the measurements. Gold electrodes with a 0.5 mm spacing were sputtered onto the surface. An alloy ingot of  $\text{Al}_{70.5}\text{Pd}_{21}\text{Re}_{8.5}$  was prepared by arc-melting. To obtain a single quasi-crystal phase, the ingot was annealed for 12 h at 940  $^{\circ}\text{C}$ . The sample was cut up into a disk shape and then mechanically polished with diamond (finest grade 1/4  $\mu\text{m}$ ). Details of the sample preparation will be published in a subsequent paper. Silver paste electrodes with a spacing of about 3 mm were used for the measurements. Ohmic behavior was confirmed for these specimens by measuring I–V character.

<sup>1</sup> Research fellow of the Japan Society for Promotion of Science.

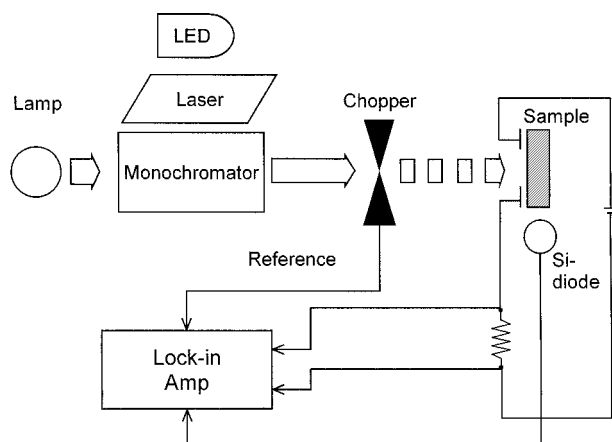


FIG. 1. Block diagram of the setup for the MPC measurement.

To measure the excitation photon energy dependence of the photocurrent for  $\beta$ -rhombohedral boron, chopped monochromatized light from a tungsten lamp was used for excitation. For frequency dependence measurements, a light emitting diode (LED) with maximum emission at 1.88 eV was used. Light from the LED was sinusoidally modulated with a function synthesizer. For the amorphous boron and the Al-Pd-Re quasicrystal, mechanically chopped light from an Ar-ion laser (2.54 eV) and a He-Ne laser (1.96 eV) were used to obtain a high S/N ratio, respectively.

A block diagram of the setup is shown in Fig. 1. The sample surface between the two electrodes was illuminated by intensity modulated monochromatic light, while illumination of the electrodes was avoided. The lock-in amplifier measured the induced photocurrent as the potential difference across a series resistance (Fig. 1). Photocurrent and phase shift were measured simultaneously. We focus on the phase shift for the analysis. As the measured phase shift also includes a phase shift due to instrumentation delay time, the actual phase shift was obtained by subtracting the phase shift of the excitation light (reference signal) measured by a fast-response Si diode with a time constant of 1 ns.

## RESULTS AND DISCUSSIONS

### Photon Energy Dependence

Figure 2 shows the photon energy dependence of the phase shift of photoconductivity in  $\beta$ -rhombohedral boron at room temperature. From absorption measurements, the band gap of  $\beta$ -rhombohedral boron was estimated to be 1.50 eV for  $E \parallel c$  and 1.46 eV for  $E \perp c$  (11). Photocurrent was observed even in the energy region lower than the band gap, and the phase shift increases with decreasing photon energy and then reaches a peak whereas no energy dependence was found in the higher energy region. In addition, the

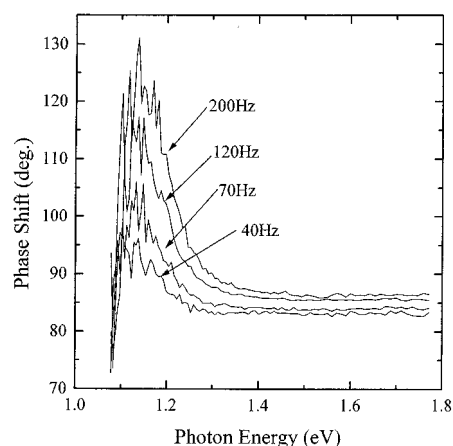


FIG. 2. Photon energy dependence of the phase shift in  $\beta$ -rhombohedral boron at room temperature. Modulated frequencies are indicated in the figure.

peak height increases and the peak position moves toward higher energy as the modulation frequency increases.

The data were analyzed by the following model (6). Figure 3 illustrates the energy band scheme and the photoconduction processes taken into account for the analysis. In this figure, the photocarrier is the electron in the conduction band, but the analysis is essentially the same when the photocarrier is the hole in the valence band. Two photocarrier generation processes are taken into consideration in the model: photoexcitation of the carrier directly to the conduction band and that directly to a localized state followed by thermal excitation into the conduction band. Unipolar photocurrent and trap-limited conduction in the conduction band are assumed.

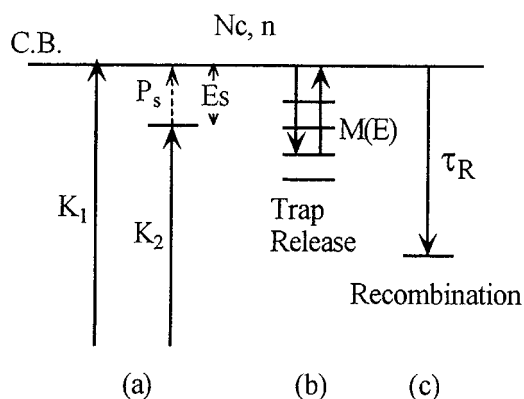


FIG. 3. Energy band scheme and photoconduction processes for the analysis; (a) photocarrier generation ( $K_1$  and  $K_2$ ), (b) interaction of carrier with localized states (trapping and release), and (c) recombination.

On the basis of the model, the concentration of excess carriers in the conduction band,  $n$ , is given by

$$n = \frac{K_1 I \tau}{\sqrt{1 + (\omega z \tau)^2}} \frac{\sqrt{\omega^2 + P_s^2 (1 + K_2/K_1)^2}}{\sqrt{P_s^2 + \omega^2}} \times \exp\{i(\omega t - \phi_1 - \phi_2)\}, \quad [1]$$

where

$$\phi_1 = \tan^{-1}(\omega z \tau) \quad [2]$$

and

$$\phi_2 = \tan^{-1} \frac{(K_2/K_1)(\omega/P_s)}{1 + (K_2/K_1) + (\omega/P_s)^2}. \quad [3]$$

In the equations,  $K_1$  and  $K_2$  are the excitation rate indicated in Fig. 3,  $I$  is the excitation photon flux,  $P_s$  is the thermal excitation rate from a localized state to the conduction band and proportional to  $\exp(-E_s/kT)$ ,  $\omega$  is the angular modulation frequency,  $\tau$  is the effective recombination time, and  $z$  is the term which relates to the interaction of carrier with localized states (trapping and release). As given in Eq. [1], the phase shift consists of two parts,  $\phi_1$  and  $\phi_2$ . Among these parameters, only  $K_1$ ,  $K_2$ , and  $P_s$  depend on the photon energy, therefore only  $\phi_2$  depends on the photon energy.

In the observed data, we regard the value of the phase shift which is independent of the photon energy in the higher energy region as  $\phi_1$ . As a result, a subtraction of the value of  $\phi_1$  from the total phase shift gives  $\phi_2$ . The results obtained for the modulation frequency of 40 and 200 Hz are shown in Fig. 4. The solid lines in Fig. 4 demon-

strate the photon energy dependence of  $\phi_2$  calculated from Eq. [3], where  $P_s = 5 \times 10^8 \exp(-(1.5 - E)/kT)$  and  $K_2/K_1 = 2.5 \exp(50(E - 1.15))$ ,  $T = 290$  K ( $E$  is the photon energy) are assumed for the calculations. The ratio of  $K_2/K_1$  is much larger than unity, and this suggests the existence of large density of localized states near the band edge of the dominant band for the conduction (valence or conduction band). The localized states are most likely to correspond to the intrinsic acceptor levels, the existence of which have been suggested from optical absorption measurements (12).

### Modulation Frequency Dependence

Figures 5, 6, and 7 show the frequency dependence of (a) photocurrent and (b) phase shift for amorphous boron,  $\beta$ -rhombohedral boron, and  $\text{Al}_{70.5}\text{Pd}_{21}\text{Re}_{8.5}$  quasicrystal, respectively. As shown in Fig. 7, we succeeded in measuring the photocurrent in the Al-Pd-Re quasicrystal for the first time. This proves the existence of a pseudogap.

Since photon energy of the excitation light used for each measurement was sufficiently large compared with the band gap of each sample, it is considered that the carrier excitation to the localized states, the process  $K_2$  in Fig. 3, can be neglected. This assumption is reasonable in usual cases. In this rather simplified model, the phase shift consists of only the  $\phi_1$  component. In Eq. [2], it is necessary to evaluate the frequency dependence of  $z\tau$ . To do this, the energetic distribution of the localized states is taken into consideration.

On the basis of the model, excess carriers,  $n$ , is given as (7)

$$n \propto \frac{I}{\sqrt{A^2 + B^2}} \exp\{i(\omega t - \phi)\}, \quad [4]$$

where

$$A = \frac{1}{\tau_R} + \int_{E_o}^{E_{fn}} v \sigma M(E) dE, \quad [5]$$

$$B = \omega + \frac{\pi}{2} k T v \sigma M(E_o), \quad [6]$$

and

$$\tan \phi = B/A. \quad [7]$$

In the equations,  $\tau_R$  is a recombination time,  $v$  is the thermal velocity,  $\sigma$  is the capture cross section for the carrier,  $M(E)$  is the density of localized states at an energy  $E$  measured from the bottom of the conduction band, and  $E_{fn}$  is the quasi-Fermi level, respectively. The energy  $E_o$  is a function of the modulation frequency and defined by

$$E_o = kT \ln(N_c v \sigma / \omega), \quad [8]$$

where  $N_c$  is an effective density of states for the conduction band. The phase shift is connected with the density of the localized states as given in Eq. [7]; therefore an energetic distribution of localized states is determined from the

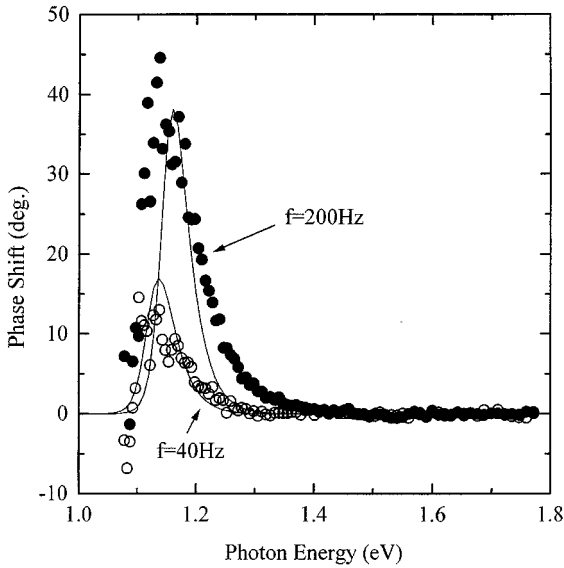


**FIG. 4.** Photon energy dependence of  $\phi_2$  in  $\beta$ -rhombohedral boron at 40 Hz (open circles) and 200 Hz (solid circles). Solid lines are calculated from Eq. [3].

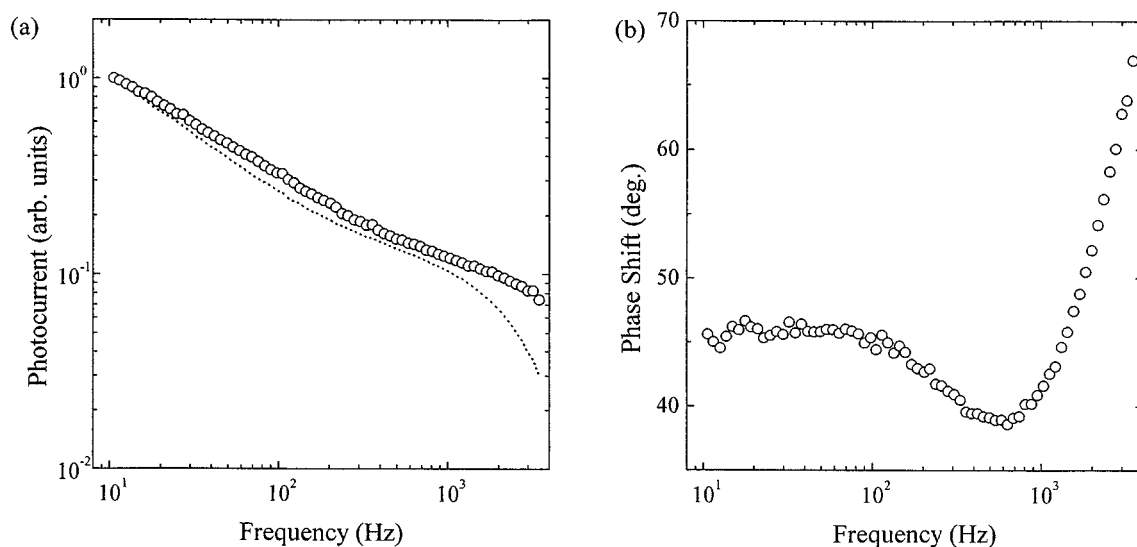


**FIG. 5.** Frequency dependence of (a) photocurrent (open circles) and (b) phase shift for amorphous boron at room temperature. The dotted line in (a) is that calculated from the phase shift (see text).

frequency dependence of the phase shift on the basis of the above equations.

The validity for applying this analysis to the observed data can be checked by comparing the observed frequency dependence of the photocurrent with that calculated from Eq. [4] using the above result of the energetic distribution of the localized states. The dotted lines in Figs. 5a, 6a, and 7a demonstrate the calculated photocurrent from these procedures. The calculated photocurrents for amorphous

boron well reproduce those observed; therefore the photoconduction process in amorphous boron can be explained by the model. Contrary to the case of amorphous boron, it is obvious that the photoconduction process both in  $\beta$ -rhombohedral boron and in the quasicrystal cannot be explained by the model.

To analyze the frequency dependence of the photocurrent for  $\beta$ -rhombohedral boron and the quasicrystal, we take the carrier excitation to the localized states,  $K_2$ , into account

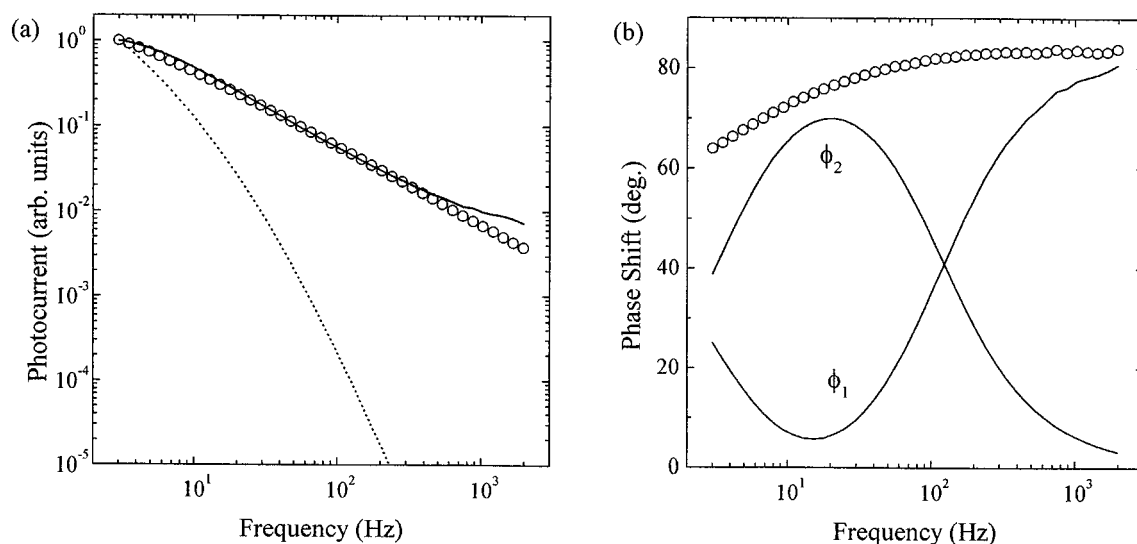


**FIG. 6.** Frequency dependence of (a) photocurrent (open circles) and (b) phase shift for  $\beta$ -rhombohedral boron at 260 K. The dotted line in (a) is that calculated from the phase shift (see text). The solid line in (a) is that calculated from Eq. [1]. The decomposition of the phase shift into  $\phi_1$  and  $\phi_2$  for the latter calculation is shown in (b).

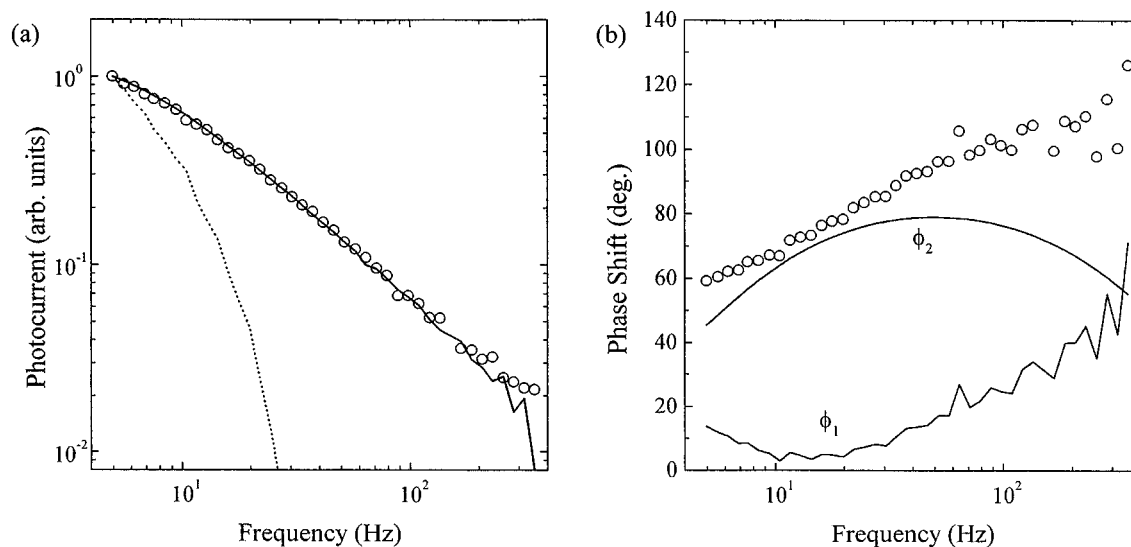


**FIG. 7.** Frequency dependence of (a) photocurrent (open circles) and (b) phase shift for  $\text{Al}_{70.5}\text{Pd}_{21}\text{Re}_{8.5}$  quasicrystal at 80 K. The dotted line in (a) is that calculated from the phase shift (see text). The solid line in (a) is that calculated from Eq. [1]. The decomposition of the phase shift into  $\phi_1$  and  $\phi_2$  for the latter calculation is shown in (b).

again, while the excitation photon energies are larger than the band gap energies of both samples. As given in Eq. [1], the observed phase shift consists of  $\phi_1$  and  $\phi_2$ . We separated the phase shift into the two parts as follows. In Eqs. [2] and [3],  $\tau$  is a frequency-dependent term whereas the other parameters in these equations are frequency independent. As a consequence, we calculate the frequency dependence of  $\phi_2$  with certain values of  $K_2/K_1$  and  $P_s$ , and then subtract the  $\phi_2$  from the observed phase shift so as to obtain the frequency dependence of  $\phi_1$ , that is, that of  $\tau$ . In the present model, to simplify the calculation, we assume one kind of localized states for the excitation process of  $K_2$ . As a result, frequency dependence of  $\phi_2$  is uniquely determined by  $K_2/K_1$  and  $P_s$ . At the low-frequency region, where the thermal excitation rate  $P_s$  is greater than the modulation frequency, the photocurrent arising from  $K_2$  shows no significant phase lag, whereas the photocurrent gradually delays as the frequency approaches  $P_s$ . At the high-frequency region, contribution of the  $K_2$  process decreases as compared with  $K_1$  which has no thermal excitation in generating photocarriers, so that  $\phi_2$  decreases with increasing frequency, although the phase shift arising from the  $K_2$  process increases. The frequency dependence of the photocurrent is calculated from Eq. [1] using the determined parameters and compared with that observed. This procedure has been finished when a good coincidence between the calculated and the observed value has been obtained.

The phase shifts in  $\beta$ -rhombohedral boron and quasicrystal are decomposed into two parts,  $\phi_1$  and  $\phi_2$ , as shown as solid lines in Figs. 6b and 7b, respectively. The calculated photocurrents are illustrated as solid lines in Figs. 6a and 7a, and these well reproduce those observed. The results

indicate that the photocarrier generation through the localized states makes a large contribution to the photoconduction process even if the excitation photon energy is larger than the band gap energy. It is considered that such behavior arises from the existence of a large density of the localized states within the gap, that is, the intrinsic acceptor levels for  $\beta$ -rhombohedral boron and the localized states within the pseudogap for the quasicrystal.

## CONCLUSION

The frequency dependence of the photocurrent for amorphous boron was explained by a rather simple model in which band-to-band excitation is assumed as the photocarrier generation process. This situation is the same as those in other amorphous semiconductors.

In contrast, the behavior of the photocurrent in  $\beta$ -rhombohedral boron and Al-Pd-Re quasicrystal were well explained by the model in which photocarrier generation via localized states is taken into consideration. For  $\beta$ -rhombohedral boron, the localized states are most likely to correspond to the intrinsic acceptor levels. For the quasicrystal, the present results strongly suggest the existence of a pseudogap at the Fermi level and a localization tendency near the Fermi level.

## ACKNOWLEDGMENTS

Two of the authors (M. Takeda and R. Tamura) acknowledge research fellowships of the Japan Society for the Promotion of Science for Young Scientists. This work has been supported by a Grant-in-Aid from the Ministry of Education, Science and Culture.

## REFERENCES

1. A. F. Hebard, M. J. Rosseinsky, R. C. Haddon, D. W. Murphy, S. H. Glarum, T. T. M. Palstra, A. P. Ramirez, and A. R. Kortan, *Nature* **350**, 600 (1991).
2. K. Kimura, H. Matsuda, R. Tamura, M. Fujimori, R. Schmechel, and H. Werheit, in "Proc. 5th Int. Conf. Quasicrystals" (C. Janot and R. Mosseri, Eds.), p. 72. World Scientific, Singapore, 1995.
3. K. Kimura and S. Takeuchi, in "Quasicrystals: The State of the Art, Directions in Condensed Matter Physics, Vol. 11" (D. P. Divinco and P. J. Steinhardt, Eds.), p. 313. World Scientific, Singapore, 1991.
4. M. Takeda, K. Kimura, A. Hori, H. Yamashita, and H. Ino, *Phys. Rev. B* **48**, 13159 (1993).
5. H. Werheit, R. Schmechel, K. Kimura, R. Tamura, and T. Lundström, *Solid State Commun.* **97**, 103 (1996).
6. H. Oheda, *Solid. State. Commun.* **33**, 203 (1980).
7. H. Oheda, *J. Appl. Phys.* **52**, 6693 (1981).
8. R. Brüggemann, C. Main, J. Berkin, and S. Reynolds, *Philos. Mag. B* **62**, 29 (1990).
9. P. Kounavis and E. Mytilineou, *J. Non-Cryst. Solids* **137&138**, 955 (1991).
10. A. Hori, M. Takeda, H. Yamashita, and K. Kimura, *J. Phys. Soc. Jpn.* **64**, 3496 (1995).
11. H. Werheit, M. Laux, and U. Kuhlmann, *Phys. Stat. Sol. (b)* **176**, 415 (1993).
12. R. Franz and H. Werheit, in "Boron-Rich Solids" (D. Emin, T. Aselage, A. C. Switendick, B. Morosin, and C. L. Beckel, Eds.), AIP Conf. Proc. 231, Am. Inst. of Physics, New York, 1991.